GSA Data Repository 2020064

Sardar Abadi, M., et al., 2020, Atmospheric dust stimulated marine primary productivity during Earth's penultimate icehouse: Geology, v. 48, https://doi.org/10.1130/G46977.1

Table DR1. Functional group assignments for taxa/ categories described for point-counted thin sections.

Functional group	Taxa/ category	Total count	Percent of total count
Autotrophic	Cyanobacteria	1476	8.50%
	Clotted micrite	1981	11.41%
	Tubiphyte	80	0.46%
	Chlorophyte	1669	9.61%
	Phylloid algae	158	0.91%
	Rhodophyte	170	0.98%
	Encrustation	2157	12.43%
Symbiont	Fusulinid	1701	9.80%
Heterotroph	Foraminifera	304	1.75%
	Coral	59	0.34%
	Crinoid	1470	8.47%
	Brachiopod	1990	11.46%
	Bryozoan	470	2.71%
	Gastropod	134	0.77%
Abiotic	Peloid	342	1.97%
	Micrite (non-clotted)	1440	8.30%
	Marine cement	72	0.41%
	Ooid	1359	7.83%
	Intraclast	327	1.88%

Table DR2. Facies description and interpretation.

Facies	Bedding and sedimentary structures	Microscopic features	Components Biotic	Components Abiotic	Occurrence and %	Depositional environments
Mid-ramp Facies Association						
F1: Fenestrate bryozoan – *Tubiphytes* boundstone	Medium to thick bedded, structureless	Clotted micrite	*Tubiphytes*, clotted micrite, red algae, green algae, Cyanophyta, small foraminifers, rare crinoids	Peloids	36% of the Moscovian interval	Within the photic zone but beneath the fair-weather wave base (mid-ramp setting)
F2: Phylloid algal packstone	Thin to medium bedded, massive, bedding thickness increases upward	broken to abraded bioclasts, poorly sorted,	Phylloid algae, Red algae, green algae, Cyanobacteria (e.g., Girvanella sp.), foraminifera, uncommon crinoid, fenestrate bryozoa	Peloids, coated grains, thick micrite envelopes	5.3% of the Moscovian interval	Within the photic zone but beneath fair-weather wave base (mid-ramp setting)
F3: Small foraminiferal packstone-grainstone	Medium to thick bedded, massive	Broken to abraded bioclasts, remobilization, poor to moderately sorted,	Foraminifera, gastropods, green algae, cyanobacteria, crinoid, rare brachiopods	Peloids, coated grains, thick micrite envelopes	11% of the Moscovian interval	Shallow marine area, under moderate energy conditions, the deposits were associated with algal meadows of F2
F4: Calcareous siltstone	Thin to medium bedded, light blue, hummocky cross-stratification	Poorly to moderately sorted, bioclasts are strongly fragmented, lamination	Brachiopod, bryozoan	Quartz	12.6% of the Asselian interval	Within to above storm wave base
F5: Brachiopod – bryozoan packstone	Medium to thick bedded, massive to cross stratified	Articulated to disarticulated brachiopods, poorly to moderately sorted, laminae	Brachiopod, bryozoan, fusulinid, crinoid, algae	Quartz	22.1% of the Asselian interval	Low- to high-energy, open marine environment, below FWWB
Inner-ramp Facies Association						
F6: Bioclastic packstone - grainstone	Thin to medium bedded, massive to planar cross–stratified (<50 cm)	Broken bioclasts, commonly encrusted by microbes, remobilization, poorly to moderately sorted	Foraminifera, gastropods, green algae, red algae, crinoid, brachiopods, coral, fusulinid	Peloids (irregularly shaped), coated grains, thick micrite envelopes, ooids (w/tangential and radial coatings, and bioclast/ quartz cores)	15.3% of the Moscovian interval; 27.4% of the Asselian interval	Skeletal shoals, deposited at or above FWWB

F7: Oolitic grainstone – packstone	Medium to thick bedded, light grey, cross stratified	Bioclasts are abraded and rounded, well sorted	Rare foraminifers, beresellis, fusulinids, crinoid	Ooids (cores of micitic grains, quartz)	26.5% of the Moscovian interval	Oolitic shoals, formed under agitated and supersaturated water conditions within foreshore
F8: Oncolitic packstone	Medium to thick bedded, massive	Broken bioclasts, commonly encrusted by microbes, bioclasts are rounded, symmetrical coated grains, moderately sorted	*Girvanella*, fusulinid, crinoid, brachiopod	Oncoids, quartz	28.5% of the Asselian interval	High-energy, well-agitated, shallow to open marine environment
F9: Calcareous mudstone - wackestone	Thin to medium bedded, massive	Bioturbation, fenestrate fabric, no lamination	Fusulinid	Quartz, peloids	9.3% of the Asselian interval	Low-energy condition, restricted environment
F10: Sandstone - siltstone	Thin to medium bedded, light grey, trough cross-stratification (<50 cm), lamination	Erosional surfaces		Quartz, ooids	%8 of the Moscovian interval	Moderate to high energy conditions, shallow subtidal to intertidal environments

Supplemental data set with iron speciation, ICP-MS results, and grain-size analysis

2020064_Dataset.xlsx

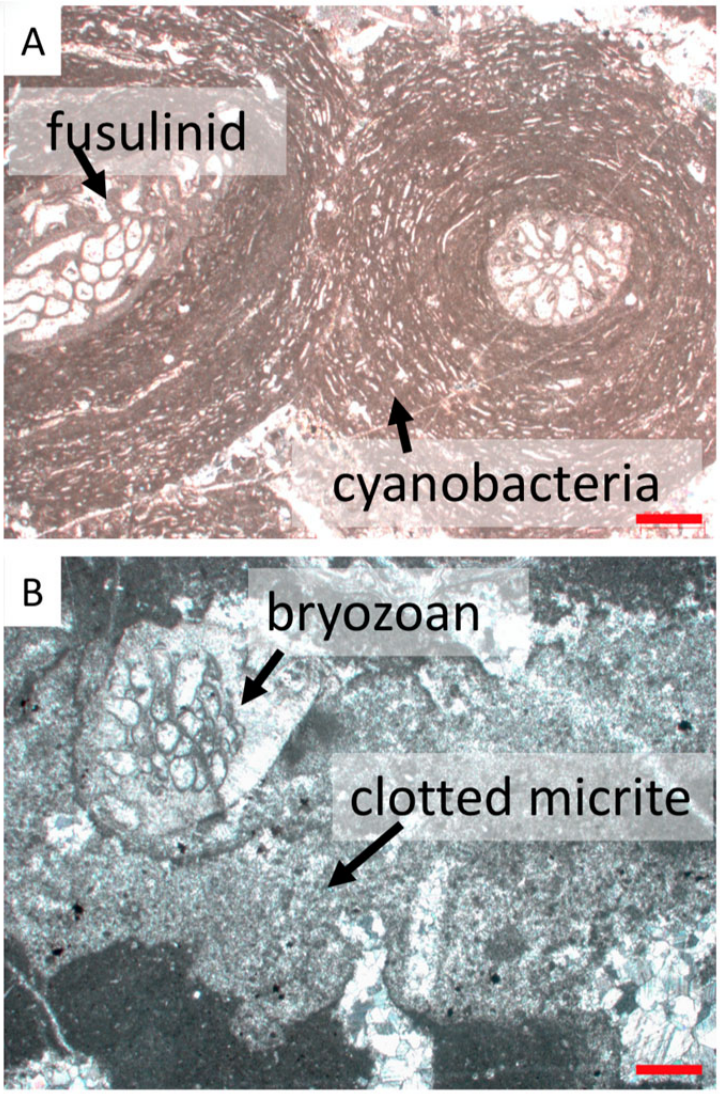

Figure DR1. Representative carbonate fossils in the studied intervals. Red scale bars = 0.5 mm. A. cyanobacterial filaments surrounding fusulinids in oncoids within the Lower Permian. B. clotted micrite fabric in association with a bryozoan fragment.

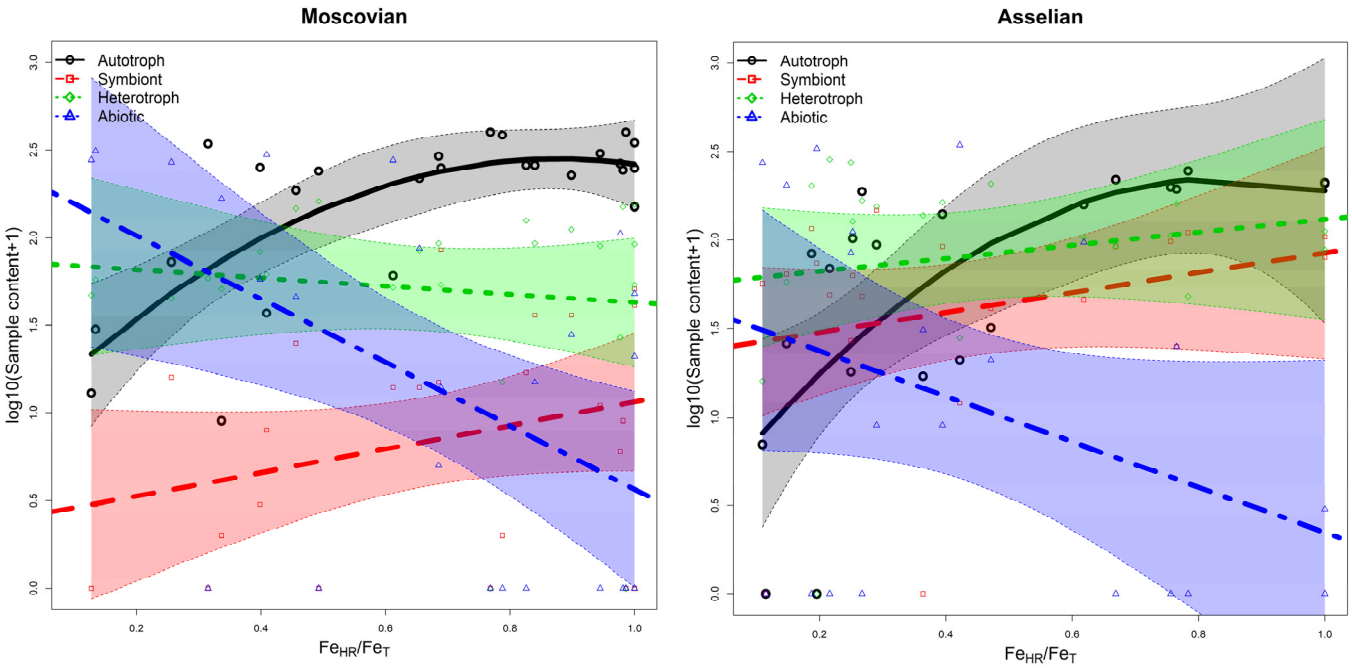

Figure DR2. The relationship between the proportion of highly reactive Fe over total Fe (Fe_{HR}/Fe_T) and log+1 transformed count of number of points containing autotrophs, symbionts, heterotrophs and abiotic content exhibits the same pattern for both the Moscovian and Asselian intervals; therefore, these two are combined as Figure 2 in the manuscript.

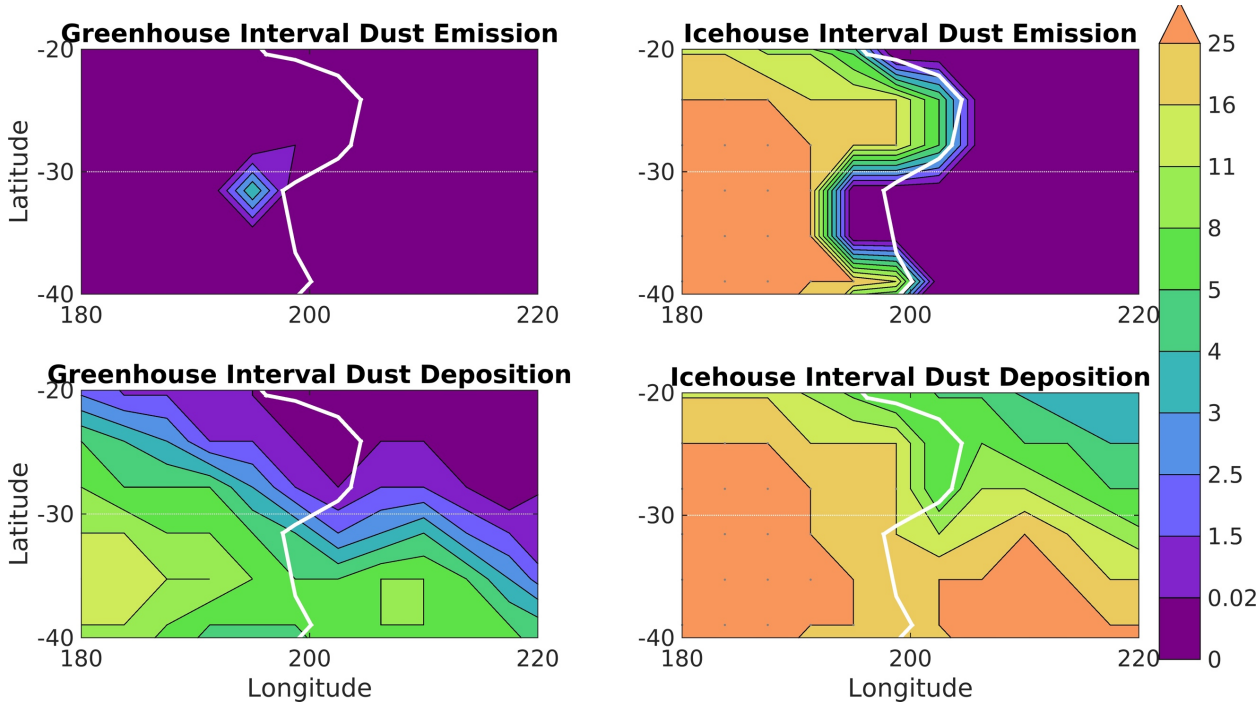

Figure DR5. Dust emission and deposition model for northeastern Gondwana margin. Dust emission and deposition in the studied area according to the reconstructions presented in Marshall et al. (2016). These reconstructions are based on climate simulations with active dust lifting and transport, but both are scaled to Marshall et al. (2016) maximum inferred dust deposition rate in Brazil (Sakmarian) The coastlines are marked by the 10% land fraction contour as opposed to the 50% land fraction contour used in Marshall et al. (2016). According to this model, dust deposition in the studied area is highly sensitive to climate, particularly to dust emission in Arabia, which the model predicts is quite low in warmer global climates and increases during colder global climates.

ICP–MS analysis:
With the total digest samples there were two sample splits of USGS SCo-1 geostandard analyzed for the entire process. Samples for this study were limited and thus did not enable duplicate analysis given the range of analyses. The reported Fe and Al data for the geostandards was within 4% of the average reported data. The sequential Fe method does not generally report a geostandard (Poulton and Canfield 2005). However, the lab has analyzed duplicate samples from previous publications that were analyzed in two different labs (Lyons – UC Riverside and Gill – Virginia Tech) and each extraction concentration has less than 6% error and the combined FeHR data is equal to or less than 5% error. Additionally, this method has been replicated in many labs around the world and it is generally accepted that the standard replication for each analysis is 7% but the entire method is better than 5%. The replication of analysis was shown in Poulton and Canfield (2005).

Organic geochemical analysis:
Rock samples were cleaned by removing the weathered surface and washed with DI water and methanol, then ground into fine powder with a pastel and mortar. Total lipid extracts (TLEs) were extracted using 1:1 dichloromethane/methanol in ultrasonic bath for 10 minutes and repeated for three times. After centrifugation the organic phase was combined and dried under a flow of nitrogen. Before analysis the TLEs were fractionated using silica gel packed in a pipette. The non-polar fraction was eluted using hexane: dichloromethane (4:1 v/v), while the polar fraction was eluted using dichloromethane:methanol (4:1 v/v). The non-polar fraction, after re-concentration in hexane, was measured using an Agilent gas chromatographer (7890B) coupled to an Agilent triple quadrupole MS/MS (7010). A multi-mode injector was installed with an initial temperature of 45C, ramped at a rate of 700C/min to a final temperature of 330C. A DB-5MS column (60m×0.25mm × 0.25um) was installed with oven temperature held at 40C for 2mins, ramped at a rate of 4C/min to a final temperature of 325 and held for 20mins. The ion source and quadrupole were set at 250C and 150C. The electron energy was set at 50eV. Biomarkers, including hopanes and methylhopanes, were acquired under multiple reaction monitoring mode.